

Coordinatively Unsaturated Hydridoruthenium(II) Complexes of N-Heterocyclic Carbenes

Kamaluddin Abdur-Rashid, Terry Fedorkiw, Alan J. Lough, and Robert H. Morris*

Davenport Laboratory, Department of Chemistry, University of Toronto, 80 St. George Street, Toronto, Ontario M5S 3H6, Canada

Received September 18, 2003

The saturated imidazolin-2-ylidene compounds $\text{RNC}_3\text{H}_4\text{NR}$, with R = mesityl (SIMes), 2,6-diisopropylphenyl, were synthesized by use of diamines that were prepared by the hydrogenation of the corresponding diimines catalyzed by $\text{RuHCl}(\text{R-binap})(\text{R,R-dach})/\text{KO}^t\text{Bu}$ in toluene. The ligands IMes ($\text{MesNC}_3\text{H}_2\text{NMe}$) and SIMes react with $\text{RuHCl}(\text{PPh}_3)_3$ to give $\text{RuH}(\text{SIMes-H})(\text{PPh}_3)_2$ (**1**) and $\text{RuH}(\text{IMes-H})(\text{PPh}_3)_2$ (**2**), respectively, where there is cyclometalation of a C–H bond of an ortho Ar–CH₃ group. The reaction of $\text{RuHCl}(\text{PPh}_3)_3$ with ^tBu ($^t\text{BuNC}_3\text{H}_2\text{N}^t\text{Bu}$) produces $^t\text{Bu}\cdot\text{HCl}$ and a red solution that, upon reaction with H₂, produces the dihydride $\text{Ru}(\text{H})_2(^t\text{Bu})(\text{PPh}_3)_2$ as a mixture of the two isomers **3a** (trans PPh₃ ligands) and **3b** (cis PPh₃). These isomers have an agostic C–H bond from a methyl group. There is an interesting windshield wiper exchange of coordinated *tert*-butyl groups occurring in isomer **3a**, as monitored in solution by VT NMR with a free energy of activation of 11.8 kcal/mol. The reaction of **2** with CO at 20 °C produces (*OC*-34)- $\text{RuH}(\text{CO})(\text{PPh}_3)_2(\text{IMes-H})$ (**4**), while at 68 °C it forms the Ru(0) complex $\text{Ru}(\text{CO})_3(\text{PPh}_3)(\text{IMes})$ (**5**). The reaction of **2** with phenol results in the formation of $\text{RuH}(\eta^5\text{-C}_6\text{H}_5\text{O}\cdot\text{HOPh})(\text{IMes})(\text{PPh}_3)$ (**6**). The structures of complexes **1**, **3a**, **5**, and **6** have been characterized by single-crystal X-ray diffraction.

Introduction

There is much current interest in the use of N-heterocyclic carbenes as ligands in homogeneous catalysts.^{1–4} The best known ruthenium catalysts of this type have been applied to olefin metathesis,^{5–8} although they have also been used for hydrogenation of alkenes⁹ and the transfer hydrogenation of ketones and a ketimine.¹⁰ The use of ruthenium catalysts in tandem reactions—first metathesis and then hydrogenation of a polyolefin¹¹ or polyketone¹²—is also of much interest.

The hydrogenation catalysts must involve hydride intermediates, but few hydridoruthenium complexes

containing N-heterocyclic carbenes are known. These include the 5-coordinate hydrogenation catalyst $\text{RuH}(\text{CO})\text{Cl}(\text{PCy}_3)(\text{IMes})$ (IMes = 1,3-bis(2,4,6-trimethylphenyl)imidazol-2-ylidene, see Chart 1),⁹ the cationic complex $[\text{RuH}(\text{C}_6\text{H}_{12}\text{N}_3)(\text{OSO}_2\text{CF}_3)(\text{PCy}_3)_2][\text{SO}_3\text{CF}_3]$,¹³ and interesting 6-coordinate complexes involved in C–H and C–C bond-breaking reactions: (*OC*-43)¹⁴- $\text{Ru}(\text{H})_2(\text{PPh}_3)_2(\text{CO})(\text{IMes})$, (*OC*-44)- $\text{Ru}(\text{H})_2(\text{IMes})_2(\text{CO})(\text{PPh}_3)$, (*OC*-53)- $\text{Ru}(\text{PPh}_3)_2(\text{IMes-H})(\text{CO})\text{H}$ (see Chart 1), and (*OC*-14)- $\text{Ru}(\text{PPh}_3)_2(\text{IMes-Me})(\text{CO})\text{H}$.¹⁵ The ligand abbreviation IMes-H indicates that this ligand is cyclometalated at a mesityl methyl group with loss of hydrogen to produce a Ru–CH₂–aryl linkage (Chart 1), while IMes-Me indicates that there is cyclometalation at a mesityl arene carbon with loss of a methyl to produce a Ru–aryl linkage.¹⁵ Other hydridoruthenium carbene complexes include the catalysts $\text{RuHCl}(\text{PR}_3)_2[\text{C}(\text{X})\text{C}_3\text{H}_6]$ (R = ⁱPr, Cy; X = O, NH) for the ring-opening metathesis polymerization of 2-norbornene^{16,17} and the useful starting vinylidene hydride $\text{RuHCl}(\text{C}=\text{CH}_2)(\text{PCy}_3)_2$.¹⁸

* To whom correspondence should be addressed. E-mail: rmorris@chem.utoronto.ca.

- (1) Trnka, T. M.; Grubbs, R. H. *Acc. Chem. Res.* **2001**, *34*, 18–29.
- (2) Weskamp, T.; Kohl, F. J.; Hieringer, W.; Gleich, D.; Herrmann, W. A. *Angew. Chem., Int. Ed.* **1999**, *38*, 2416.
- (3) Grubbs, R. H. *Adv. Synth. Catal.* **2002**, *344*, 569–569.
- (4) Herrmann, W. A. *Angew. Chem., Int. Ed.* **2002**, *41*, 1290–1309.
- (5) Jafarpour, L.; Hillier, A.; Nolan, S. *Organometallics* **2002**, *21*, 442–444.
- (6) Bielawski, C. W.; Benitez, D.; Grubbs, R. H. *Science* **2002**, *297*, 2041–2044.
- (7) Furstner, A.; Ackermann, L.; Gabor, B.; Goddard, R.; Lehmann, C. W.; Mynott, R.; Stelzer, F.; Thiel, O. R. *Chem. Eur. J.* **2001**, *7*, 3236–3253.
- (8) Denk, K.; Fridgen, J.; Herrmann, W. A. *Adv. Synth. Catal.* **2002**, *344*, 666–670.
- (9) Lee, H. M.; Smith, D. C.; He, Z. J.; Stevens, E. D.; Yi, C. S.; Nolan, S. P. *Organometallics* **2001**, *20*, 794–797.
- (10) Danopoulos, A. A.; Winston, S.; Motherwell, W. B. *Chem. Commun.* **2002**, *80*, 1376–1377.
- (11) Drouin, S. D.; Zamanian, F.; Fogg, D. E. *Organometallics* **2001**, *20*, 5495–5497.
- (12) Louie, J.; Bielawski, C. W.; Grubbs, R. H. *J. Am. Chem. Soc.* **2001**, *123*, 11312–11313.

- (13) Chaumonnot, A.; Donnadiou, B.; Sabo-Etienne, S.; Chaudret, B.; Biron, C.; Bertrand, G.; Metivier, P. *Organometallics* **2001**, *20*, 5614–5618.

(14) For the stereochemical descriptors see: Geoffroy, G. L., *Inorganic and Organometallic Stereochemistry*. In *Topics in Stereochemistry*; Allinger, N. L., Eliel, E. L., Eds.; Wiley: New York, 1981; Vol. 12.

(15) Jazzar, R. F. R.; Macgregor, S. A.; Mahon, M. F.; Richards, S. P.; Whittlesey, M. K. *J. Am. Chem. Soc.* **2002**, *124*, 4944–4945.

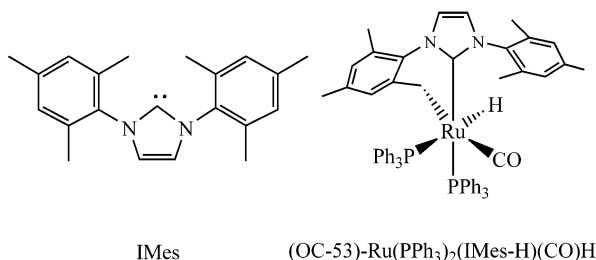
(16) Coalter, J. N.; Caulton, K. G. *New J. Chem.* **2001**, *25*, 679–684.

(17) Ferrando-Miguel, G.; Coalter, J. N.; Gerard, H.; Huffman, J. C.; Eisenstein, O.; Caulton, K. G. *New J. Chem.* **2002**, *26*, 687–700.

(18) Jung, S.; Ilg, K.; Wolf, J.; Werner, H. *Organometallics* **2001**, *20*, 2121–2123.

Table 1. Selected Crystal Data and Data Collection and Refinement Parameters for 1, 3a, 5, and 6

	1	3a	5	6
formula	C ₅₇ H ₅₆ N ₂ P ₂ Ru	C ₄₇ H ₅₂ N ₂ P ₂ Ru	C ₄₆ H ₄₇ O ₄ N ₂ PRu	C ₅₁ H ₅₁ O ₂ N ₂ PRu
<i>M_r</i>	932.05	807.92	823.90	855.98
cryst syst	triclinic	triclinic	monoclinic	monoclinic
space group	<i>P</i> 1	<i>P</i> 1	<i>P</i> 2 ₁ / <i>n</i>	<i>P</i> 2 ₁ / <i>n</i>
<i>a</i> , Å	11.2350(2)	9.1155(1)	11.2770(9)	15.0950(2)
<i>b</i> , Å	11.6468(2)	10.3552(1)	12.446(1)	11.0320(2)
<i>c</i> , Å	18.6606(4)	12.5275(2)	29.068(3)	26.2100(4)
α, deg	80.145(1)	106.318(1)	90.00	90.00
β, deg	78.027(1)	111.090(1)	96.445(3)	105.6740(7)
γ, deg	86.100(1)	95.1280(10)	90.00	90.00
<i>V</i> , Å ³	2352.07(8)	1034.62(2)	4054.0(6)	4202.40(11)
<i>Z</i>	2	1	4	4
ρ _{calcd} , g cm ⁻³	1.316	1.297	1.350	1.353
μ(Mo, Kα), mm ⁻¹	0.441	0.490	0.471	0.454
<i>F</i> (000)	972	422	1712	1784
cryst size, mm ³	0.28 × 0.30 × 0.34	0.23 × 0.20 × 0.15	0.15 × 0.06 × 0.04	0.30 × 0.20 × 0.08
θ range, deg	2.6–27.5	2.87–27.58	2.60–25.13	2.58–27.49
no. of rflns collected	27 554	12 007	18 029	25 600
no. of indep rflns	10 769 (<i>R</i> _{int} = 0.031)	7566 (<i>R</i> _{int} = 0.032)	7104 (<i>R</i> _{int} = 0.1195)	9580 (<i>R</i> _{int} = 0.0456)
abs cor		semiempirical from equivalents		
max and min transmission coeff	0.8864 and 0.08644	0.9301 and 0.8956	0.994 and 0.780	0.968 and 0.895
no. of params refined	569	482	494	523
GOF on <i>F</i> ²	1.041	1.040	1.070	1.035
<i>R</i> 1 ^a (<i>I</i> > 2σ(<i>I</i>))	0.0315	0.0238	0.0962	0.0384
w <i>R</i> 2 ^b (all data)	0.0778	0.0574	0.2536	0.0916
peak and hole, e Å ⁻³	0.449 and -0.572	0.360 and -0.459	0.849 and -0.639	0.636 and -0.887

Chart 1. The IMes Ligand and the Complex (OC-53)-Ru(PPh₃)₂(IMes-H)(CO)H¹⁵

This work describes an alternative preparation of N-heterocyclic carbene ligands involving the first use of an imine hydrogenation catalyst to prepare the precursor to the saturated ligand SIMes and its analogues. These ligands have been used to prepare some novel ruthenium hydrido complexes.

Experimental Section

General Considerations. Unless otherwise stated, all preparations and manipulations were carried out under a purified H₂, N₂, or Ar atmosphere with the use of standard Schlenk, vacuum line, and glovebox techniques in dry, oxygen-free solvents. Tetrahydrofuran (THF), diethyl ether, and hexanes were dried and distilled from sodium–benzophenone ketyl. Deuterated solvents were degassed and dried over molecular sieves. C₆D₆ was obtained from Cambridge Isotope Laboratories and dried by storing over molecular sieves (3A, beads, 8–12 mesh, Aldrich Chemical Co.). ¹H NMR spectra for variable-temperature analysis were recorded on a Varian Unity 500 spectrometer (500 MHz for ¹H). All other NMR spectra were obtained on a Varian Gemini 300 MHz spectrometer (300 MHz for ¹H and 121.5 MHz for ³¹P). All ³¹P spectra were recorded with proton decoupling, and ³¹P chemical shifts were measured relative to 85% H₃PO₄ as an external reference. ¹H chemical shifts were measured relative to partially deuterated solvent peaks but are reported relative to tetramethylsilane. Infrared spectra were obtained on a Nicolet 550 Magna-IR spectrometer or a Perkin-Elmer Paragon 500 FT-IR spectrometer.

Single-crystal X-ray diffraction data were collected using a Nonius Kappa-CCD diffractometer with Mo Kα radiation (λ = 0.710 73 Å). The CCD data were integrated and scaled using the Denzo-SMN package. The structures were solved and refined using SHELXTL V5.1. Refinement was by full-matrix least squares on *F*² using all data (negative intensities included). Hydride atoms were located and refined with isotropic thermal parameters. Details are listed in Table 1. The crystals of 5 were fine needles, and there was a partially disordered THF in the lattice. This resulted in a structure with lowered precision.

Unless otherwise stated, all chemicals were purchased from Sigma Aldrich. The following compounds were prepared by literature methods: RuHCl(PPh₃)₃,¹⁹ glyoxalbis(2,4,6-trimethylphenyl)imine, glyoxalbis(2,6-diisopropylphenyl)imine, 1,3-bis(2,4,6-trimethylphenyl)imidazolin-2-ylidene (SIMes), 1,3-bis(2,4,6-trimethylphenyl)imidazol-2-ylidene (IMes),²⁰ and RuH(Cl)(*R*-binap)(*R*,*R*-dach) (dach = cydn = diaminocyclohexane).²¹ However, the diamine dihydrochloride starting material for SIMes was prepared as described below and the imidazolium precursors for the carbenes were made on a smaller scale (2 g) than reported,²⁰ with a shorter reaction time (1–2 h at reflux in THF) for the IMes precursor. The carbenes were produced by reaction of the imidazolium salts with pure KH in THF at room temperature (Scheme 1). Nitrogen gas (prepurified grade), argon gas (ultrahigh purity grade), hydrogen gas (grade 4.0), and carbon monoxide (industrial grade) were obtained from BOC Gases Canada and used without further purification.

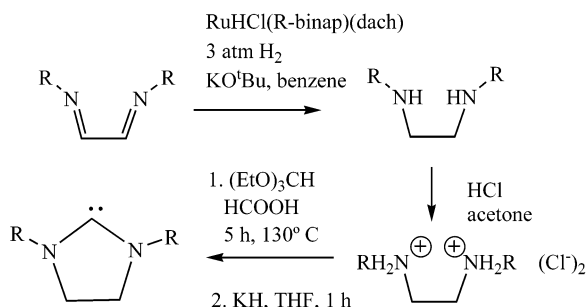
***N,N*-Bis((2,4,6-trimethylphenyl)amino)ethane Dihydrochloride.**²⁰ Under a flow of N₂, a suspension of glyoxalbis(2,4,6-trimethylphenyl)imine (2 g, 6.8 mmol), RuHCl(*R*-binap)-(*R*,*R*-cydn) (0.01 g, 0.01 mmol), and potassium *tert*-butoxide (0.03 g, 0.03 mmol) was prepared in toluene. The suspension was stirred under 3 atm of H₂ gas for 6 h, during which time the yellow solid dissolved. To the solution was added 2 mL of concentrated hydrochloric acid. Upon addition of acetone, a

(19) Schunn, R. A.; Wonchoba, E. R.; Wilkinson, G. *Inorg. Synth.* **1971**, *13*, 131–134.

(20) Arduengo, A. J., III; Krafczyk, R.; Schmutzler, R.; Craig, H. A.; Goerlich, J. R.; Marshall, W. J.; Unverzagt, M. *Tetrahedron* **1999**, *55*, 14523–14534.

(21) Abdur-Rashid, K.; Lough, A. J.; Morris, R. H. *Organometallics* **2001**, *20*, 1047–1049.

Scheme 1. New Synthetic Route to Saturated Carbenes (R = Mesityl (SIMes), 2,6-Diisopropylphenyl)



colorless solid precipitated and was collected by filtration and dried in vacuo. Yield: 2.13 g (86%). ^1H NMR (DMSO- d_6): δ 2.20 (s, 6H, *p*-CH₃), 2.39 (s, 12H, *o*-CH₃), 3.50 (s, 4H, NCH₂), 6.91 (s, 4H, *m*-CH). $^{13}\text{C}\{^1\text{H}\}$ NMR (DMSO- d_6): δ 18.17 (s, *o*-CH₃), 20.28 (s, *p*-CH₃), 46.71 (s, NCH₂), 130.0 (s, *ipso*-C), 131.2 (s, *m*-C), 135.0 (s, *o*-C), 135.7 (s, *p*-C).

***N,N*-Bis(2,6-diisopropylphenyl)aminoethane Dihydrochloride.**²⁰ The same method and conditions were used as above. Yield: 1.95 (85%). ^1H NMR (DMSO- d_6): δ 1.18 (d, 24H, CH(CH₃)₂, $^3J_{\text{HH}} = 6.6$ Hz), 3.43 (sept, 4H, CH(CH₃)₂, $^3J_{\text{HH}} = 6.6$ Hz), 3.46 (s, 4H, NCH₂), 7.27 (m, 6H, aryl CH). $^{13}\text{C}\{^1\text{H}\}$ NMR (DMSO- d_6): δ 25.15 (s, CH(CH₃)₂), 27.92 (s, CH(CH₃)₂), 50.02 (s, NCH₂), 125.7 (s, *m*-C), 128.1 (s, *p*-C), 142.1 (s, *o*-C), 143.4 (s, *ipso*-C).

RuH(SIMes-H)(PPh₃)₂ (1). In a glovebox, a Schlenk flask was charged with RuHCl(PPh₃)₃ (500 mg, 0.54 mmol), 1,3-bis-(2,4,6-trimethylphenyl)imidazolin-2-ylidene (350 mg, 1.14 mmol), and 1 mL of THF. The mixture was refluxed under a flow of N₂ for 12 h. It was then filtered to remove SIMes-HCl. Hexanes (5 mL) was added to the filtrate to precipitate the product, which was then collected by filtration, washed with hexanes, and dried under vacuum. Crystals suitable for X-ray measurements were obtained by slow diffusion of hexanes into a saturated THF solution of the complex under Ar. Yield: 435 mg (85%). ^1H NMR (C₆D₆): δ 7.46–6.7 (m, 32H, Ar H), 6.60 (m, 1H, *m*-Ar H), 5.08 (s, 1H, Ar-H ortho to C19 of Figure 1, shielded by cis Ph–P ring), 3.60 (m, 2H, NCH₂), 3.38 (m, 3H, NCH₂ and 1H of RuCH₂), 2.92 (s, 3H, CH₃), 2.46 (s, 3H, CH₃), 2.25 (m, 1H, RuCH₂), 2.21 (s, 3H, CH₃), 1.97 (s, 3H, CH₃), 1.15 (s, 3H, CH₃), –26.5 (dd, $^2J_{\text{HP}} = 24$, 27 Hz, 1H, Ru–H). $^{31}\text{P}\{^1\text{H}\}$ NMR (C₆D₆): δ 59.9 (PPh₃, A part of AB pattern, $^2J_{\text{PP}} = 13.6$ Hz), 59.3 (PPh₃, B part of AB pattern, $^2J_{\text{PP}} = 13.6$ Hz). The NMR spectrum showed the presence of traces of Ru(H)₂N₂(PPh₃)₃. Poor combustion or air sensitivity of the sample resulted in low C and N analyses on several attempts.

RuH(IMes-H)(PPh₃)₂ (2). In a glovebox, a Schlenk flask was charged with RuHCl(PPh₃)₃ (220 mg, 0.24 mmol), 1,3-bis-(2,4,6-trimethylphenyl)imidazol-2-ylidene (182 mg, 0.60 mmol), and 3 mL of THF. The mixture was stirred overnight under a flow of argon. It was then filtered to remove IMes-HCl. Hexanes (5 mL) was added to precipitate the product. The solids were filtered, washed with hexanes, and dried under vacuum. Yield: 170 mg (77%). ^1H NMR (C₆D₆): δ 7.20–6.80 (m, 30H, Ar H), 6.61 (s, 1H, *m*-Ar H), 6.43 (s, 1H, *m*-Ar H), 6.09 (s, 1H, *m*-Ar H), 5.15 (s, 1H, *m*-Ar H shielded by cis Ph–P ring as for 1), 3.80 (m, 1H of RuCH₂), 2.83 (s, 3H, CH₃), 2.43 (s, 3H, CH₃), 2.20 (m, 1H of RuCH₂), 2.20 (s, 3H, CH₃), 1.96 (s, 3H, CH₃), 0.83 (s, 3H, CH₃), –28.03 (dd, 1H, $^2J_{\text{HP}} = 25$, 28 Hz, Ru–H). $^{31}\text{P}\{^1\text{H}\}$ NMR (C₆D₆): δ 58.9 (PPh₃, A part of AB pattern, $^2J_{\text{PP}} = 12.9$ Hz), 58.3 (PPh₃, B part of AB pattern, $^2J_{\text{PP}} = 12.9$ Hz). $^{13}\text{C}\{^1\text{H}\}$ NMR (75.4 MHz, C₆D₆): aromatic, δ 140.8 (s), 140.5 (s), 137.6 (s), 137.3 (s), 137.2 (s), 135.8 (s), 135.7 (br), 135.4 (br), 135.0 (d, 8.7 Hz), 133.6 (br d, 9.0 Hz), 132.0 (br), 131.4 (d, 4 Hz), 128.9 (s), 128.8, 127.2 (d, 6.0 Hz), 126.7 (d, 6.0 Hz), 125.9 (br); imine, δ 122.8 (d, 3 Hz, CH=N), 118.9

(m, CH=N); methyl, δ 21.0 (s), 20.9 (s), 19.6 (s), 18.6 (s), 16.0 (s); Ru–C not observed. IR (Nujol): 1945 cm^{–1} (RuH). Anal. Calcd for C₅₇H₅₄N₂P₂Ru: C, 73.50; H, 5.80; N, 3.01. Found: C, 72.36; H, 6.19; N, 3.59.

RuH₂(^{*i*}Bu)(PPh₃)₂ (3a,b). In a glovebox, a Schlenk flask was charged with RuHCl(PPh₃)₃ (1.0 g, 1.1 mmol), 1,3-di-*tert*-butylimidazol-2-ylidene (400 mg, 2.2 mmol), and 2 mL of THF. The mixture was refluxed under a flow of argon for 8 h to yield a red solution. It was then filtered to remove ^{*i*}Bu·HCl, and the filtrate was then stirred under H₂ gas, whereupon the bright yellow dihydride complex instantaneously formed. It was precipitated with hexanes (5 mL), collected by filtration, washed with hexanes, and dried under vacuum. Yield: 427 mg (50%). Crystals suitable for X-ray measurements were obtained by slow diffusion of hexanes into a saturated diethyl ether solution of the complex under Ar. Two isomers, **3a,b**, were present in the ^1H NMR spectrum in a ratio of 7:3, along with minor impurity peaks. $^{31}\text{P}\{^1\text{H}\}$ NMR (C₆D₆, 20 °C): δ 64.3 (s, **3a**), 62.7 (d, $J_{\text{PP}} = 36.9$ Hz, **3b**), 51.4 (d, $J_{\text{PP}} = 36.9$ Hz, **3b**). ^1H NMR of the hydride region (toluene- d_8 , –80 °C): δ –21.14 (t, broad, **3a**), –19.75 (s, broad, **3b**), –10.55 (t, $J = 19.2$ Hz, **3a**), –5.82 (dd, $J_{\text{PH}^{\text{trans}}} = 83$ Hz, $J_{\text{HP}^{\text{cis}}} = 30.5$ Hz, **3b**). ^1H NMR, hydride region (toluene- d_8 , 50 °C): δ –20.47 (s, broad, **3b**), –16.20 (s, broad, **3a**), –6.52 (s, broad, **3b**). Anal. Calcd for C₄₇H₅₂N₂P₂Ru: C, 69.80; H, 6.44; N, 3.47. Found: C, 69.35; H, 6.51; N, 4.46.

(OC-34)-RuH(CO)(IMes-H)(PPh₃)₂ (4). A Schlenk flask was charged with **2** (200 mg, 0.21 mmol) and 3 mL of THF. The solution was stirred for 3 h at room temperature under a flow of carbon monoxide, during which time the color changed from red to light brown. Hexanes (8 mL) was added to precipitate the product, which was collected by filtration, washed with hexanes, and dried under vacuum. Yield: 155 mg (76%). $^{31}\text{P}\{^1\text{H}\}$ NMR (C₆D₆): δ 60.2 (d, PPh₃, $^2J_{\text{PP}} = 12$ Hz), 48.6 (d, PPh₃, $^2J_{\text{PP}} = 12$ Hz). ^1H NMR (C₆D₆): δ 7.8–6.8 (m, 30H, Ar H), 6.77 (s, 1H, *m*-Ar H), 6.43 (s, 1H, N–C=CH), 6.22 (s, 1H, *m*-Ar H), 6.11 (s, 1H, NC=CH), 2.87 (s, 3H, CH₃), 2.61 (br “t”, $^2J_{\text{HH}} = ^2J_{\text{PH}} = 9$ Hz, 1H of RuCH₂), 2.42 (s, 3H, CH₃), 2.25 (s, 3H, CH₃), 2.17 (s, 3H, CH₃), 1.70 (ddd, $^2J_{\text{HH}} = 9$ Hz, $^3J_{\text{PH}} = 12$, 3 Hz), 0.77 (s, 3H, CH₃), –5.20 (dd, 1H, Ru–H, $^2J_{\text{HP}} = 16$, 30 Hz). $^{13}\text{C}\{^1\text{H}\}$ NMR (C₆D₆, 75.4 MHz): δ 14.0 (s, Me), 17.8 (s, Me), 19.2, (s, Me), 20.8 (d, RuCH₂, $^3J_{\text{PC}} = 3$ Hz), 22.7 (s, Me), 124.7 (s, CH=N), 127–128 (m), 128.8 (s), 128.9 (s), 133.6 (m), 134.3 (d, 8 Hz). IR (cm^{–1}, Nujol): ν_{CO} 1949.

Ru(CO)₃(IMes)(PPh₃)₂ (5). A Schlenk flask was charged with **2** (200 mg, 0.21 mmol) and 3 mL of THF. The solution was refluxed overnight under a flow of carbon monoxide, during which time the color changed from red to yellow. Hexanes (8 mL) was added to precipitate the product, which was collected by filtration, washed with hexanes, and dried under vacuum. Yield: 155 mg (95%). Crystals suitable for X-ray measurements were obtained by slow diffusion of hexanes into a saturated THF solution of the complex under Ar. ^1H NMR (C₆D₆): δ 7.3–6.90 (m, 15H, Ar H), 6.87 (s, 1H, NC=CH), 6.27 (s, 1H, NC=CH), 2.21 (s, 12H, *o*-CH₃), 2.16 (s, 6H, *p*-CH₃). $^{31}\text{P}\{^1\text{H}\}$ NMR (C₆D₆): δ 59.0 (s, PPh₃). ^{13}C NMR (C₆D₆): δ 211.4 (d, 12.6 Hz, Ru–CO), 138.4 (s), 138.1 (s), 137.1 (s), 136.7 (s), 136.1 (s), 134.0 (d, 8.5 Hz, P–C), 129.1 (s), 129.07 (s), 127.6 (s), 122.5 (d, 2 Hz, CH=N), 20.8 (s, *p*-CH₃), 18.4 (s, *o*-CH₃). IR (cm^{–1}, Nujol): ν_{CO} 1965, 1885, 1850.

RuH(C₆H₅O·HOPh)(IMes)(PPh₃)₂ (6). In a glovebox, a Schlenk flask was charged with **2** (200 mg, 0.21 mmol), phenol (47 mg, 0.54 mmol), and 5 mL of THF. The mixture was stirred for 3 h under an atmosphere of argon, during which time the color changed from red to yellow. Hexanes (10 mL) was added to precipitate the product, which was collected by filtration, washed with hexanes, and dried under vacuum. Yield: 185 mg (92%). Crystals suitable for X-ray measurements were obtained by slow diffusion of hexanes into a saturated THF solution of the complex. ^1H NMR (C₆D₆): δ 7.3–6.80 (m, 15H, Ar H), 6.72 (s, 1H, *m*-Ar H), 6.60 (s, 1H, NC=CH) 6.35 (s, 1H,

m-Ar H), 6.13 (s, 1H, NC=CH), 5.78 (s, 1H, OC₆H₅), 5.18 (t, 1H, OC₆H₅), 5.10 (d, 1H, OC₆H₅), 4.88 (t, 1H, OC₆H₅), 4.55 (d, 1H, OC₆H₅), 2.47 (s, 3H, CH₃), 2.31 (s, 3H, CH₃), 2.28 (s, 3H, CH₃), 2.15 (s, 3H, CH₃), 2.06 (s, 3H, CH₃), 1.35 (s, 3H, CH₃), -11.90 (d, ²J_{HIP} = 44.7 Hz, 1H, Ru-H). ³¹P{¹H} NMR (C₆D₆): δ 53.2 (s, PPh₃). ¹³C NMR (C₆D₆): aromatic, δ 161.5 (s, C=O of η⁵-C₆H₅O), 156.6 (s, phenol), 138.5 (s), 138.2 (d), 137–136 (m), 134.4 (s), 133.8 (s), 129.6 (s, phenol), 127.3 (s), 124.3 (s, CH=N), 124.0 (s, CH=N), 120.0 (s, phenol), 115.7 (s, phenol); η⁵-C₆H₅O, δ 97.4 (s), 95.6 (s), 79.9 (s), 77.8 (s), 76.6 (s), 67.5 (s); methyl, δ 25.1 (s), 20.8 (s), 20.6 (s), 20.5 (s), 19.0 (s), 16.7 (s). IR (cm⁻¹, Nujol): ν_{Ru-H} 2002. Anal. Calcd for C₅₁H₅₂N₂P₂O₂-Ru: C, 71.47; H, 6.12; N, 3.27. Found: C, 71.90; H, 6.11; N, 3.50.

Results and Discussion

Catalytic Hydrogenation of Diimines in the Synthesis of Saturated Carbenes. The saturated imidazolin-2-ylidene compounds with mesityl or 2,6-diisopropylphenyl groups on nitrogen were synthesized according to Scheme 1. The compound with mesityl groups (known as SIMes) was used in subsequent reactions.

The imine hydrogenation precatalyst RuHCl(*R*-bi-*nap*)(*R,R*-dach), which is available in our laboratory,²¹ was chosen to hydrogenate the diimines of Scheme 1 in favor of the familiar Arduengo method of reduction with sodium borohydride.²⁰ The Arduengo method requires the use of a large excess of NaBH₄ and subsequent neutralization. The major advantage of our hydrogenation is the simplicity in workup of the ammonium salts. The addition of concentrated hydrochloric acid to the diamine solution that is produced from the hydrogenation reaction resulted in the rapid precipitation of the hydrochloride adducts. These could be isolated by simple filtration. Subsequent preparation of the imidazolium chloride salts and imidazolin-2-ylidene compounds followed the literature methods.²⁰

We are not aware of other reports of homogeneous catalysts used to hydrogenate diimines in this way. Other nonchiral diamine diphosphine ruthenium catalysts should also catalyze the hydrogenation of such diimines.

Ruthenium Complexes of Carbenes with Mesityl Groups. The complex RuHCl(PPh₃)₃ was reacted with two related carbenes, SIMes and IMes, as shown in Scheme 2.

The alternative method of generating the carbenes in situ by the reaction of KO^tBu with the corresponding imidazolium salt precursors and then reacting them with RuHCl(PPh₃)₃ also produced complexes **1** and **2** along with some uncharacterized side products. The complexes were characterized by multinuclear NMR spectroscopy, IR spectroscopy, and X-ray crystallography (for **1**). They are both air-sensitive red solids, soluble in THF, benzene, and diethyl ether and insoluble in hexanes.

The complex **1** has a slightly distorted square-pyramidal structure with an apical hydride (Figure 1). The ruthenium has inserted into one of the C-H bonds of an ortho Ar-CH₃ group of the SIMes ligand to yield a new Ru-C bond (Ru(1)-C(19) = 2.16(2) Å, see Table 2). An unusual feature is the Ru(1)-C(19)-C(16) angle of 89.6°, where C(16) is the ipso ring carbon attached to C(19). This might be interpreted as η²-benzyl char-

Scheme 2. Synthesis of RuH(SIMes-H)(PPh₃)₂ (**1**) and RuH(IMes-H)(PPh₃)₂ (**2**)

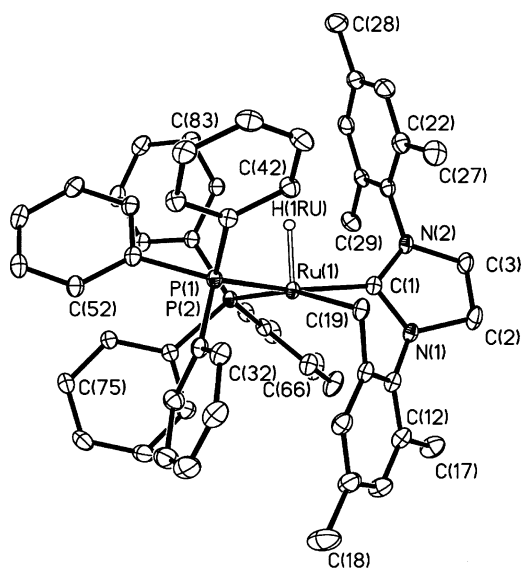
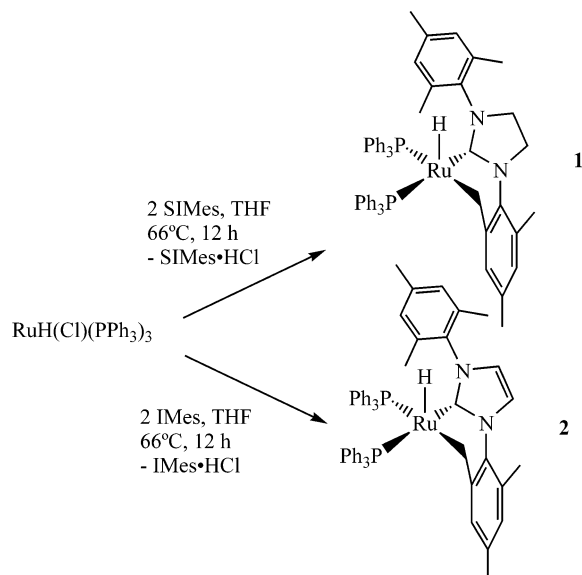


Figure 1. X-ray crystal structure of RuH(SIMes-H)(PPh₃)₂ (**1**).

Table 2. Selected Bond Distances and Angles for **1**

Bond Lengths (Å)			
Ru(1)-H(1Ru)	1.51(2)	Ru(1)-P(1)	2.3186(5)
Ru(1)-C(1)	2.045(2)	Ru(1)-P(2)	2.3110(5)
Ru(1)-C(19)	2.162(2)	C(2)-C(3)	1.505(3)
Bond Angles (deg)			
H(1Ru)-Ru(1)-C(1)	88.0(8)	P(2)-Ru(1)-P(1)	98.94(2)
H(1Ru)-Ru(1)-C(19)	104.8(8)	C(1)-Ru(1)-P(2)	98.37(5)
H(1Ru)-Ru(1)-P(2)	91.7(8)	C(1)-Ru(1)-P(1)	161.00(5)
H(1Ru)-Ru(1)-P(1)	83.7(8)		
C(1)-Ru(1)-C(19)	78.24(7)	N(1)-C(1)-N(2)	106.2(2)

acter, as observed in other complexes with acute M-CH₂-C(Ar) angles of less than 90°. However, the distance from ruthenium to the aryl carbon (Ru(1)⋯C(16) = 2.61 Å) is too long for a significant Ru-C bonding interaction.

(22) Dryden, N. H.; Legzdins, P.; Trotter, J.; Yee, V. C. *Organometallics* **1991**, *10*, 2857–2870.

(23) Rogers, J. S.; Lachicotte, R. J.; Bazan, G. C. *Organometallics* **1999**, *18*, 3976–3980.

The solution NMR properties of complexes **1** and **2** fit with the crystal structure of **1**. The ^{31}P NMR resonances are two doublets for two inequivalent phosphorus nuclei. The unusually high-field chemical shifts of the hydrides of **1** and **2** at -26.5 and -28.0 ppm, respectively, are characteristic of hydride in the apical position of square-pyramidal Ru(II) complexes.^{9,13,24,25}

The detailed mechanism of the reactions of Scheme 2 is unknown. The substitution of a phosphine ligand by carbenes of this type is thermodynamically favorable.^{5,26,27} The coordination of a mesityl methyl carbon-hydrogen bond would render it acidic and susceptible to deprotonation by a second equivalent of carbene, a strong base. Alternatively, the dehydrohalogenation²⁸ of the ruthenium complex by the carbene to yield a reactive ruthenium(0) intermediate and then oxidative addition of the methyl C-H bond might also lead to the observed product. The cyclometalation of a substituent on nitrogen of a carbene on ruthenium is a fairly common reaction.^{15,29-31}

All attempts to form a bis(carbene)ruthenium complex failed, including refluxing a THF solution of $\text{RuHCl}(\text{PPh}_3)_3$ with a 10-fold excess of a carbene, either IMes or SIMes, for 7 days. Although **1** and **2** have vacant coordination sites, they are apparently too sterically hindered to allow the addition of a second IMes ligand. The IMes ligand is larger than triphenylphosphine, at least in a two-dimensional fashion. Recently, Whittlesey and co-workers formed the bis(carbene) complex $\text{Ru}(\text{CO})(\text{H})_2(\text{IMes})_2(\text{EtOH})$, by displacing triphenylarsine ligands.³²

Reactions of 2. To see whether complex **2** can be converted into the known complex $(OC-53)\text{-RuH}(\text{CO})(\text{IMes-H})(\text{PPh}_3)_2$ (Chart 1),¹⁵ it was reacted with carbon monoxide under mild and then more forcing conditions. The reaction of $\text{RuH}(\text{IMes-H})(\text{PPh}_3)_2$ with excess carbon monoxide at room temperature resulted in the formation of the monocarbonyl-substituted product $(OC-34)\text{-RuH}(\text{CO})(\text{IMes-H})(\text{PPh}_3)_2$ (**4**), in which one carbon monoxide molecule simply coordinates to the vacant site of the 16-electron complex (Scheme 3).

$\text{RuH}(\text{CO})(\text{IMes-H})(\text{PPh}_3)_2$ is a white solid, which appears to be stable in air indefinitely. It is soluble in THF, benzene, and ether and insoluble in hexanes. The ^{31}P and ^1H NMR spectrum are consistent with the structure shown in Scheme 3, with *cis* PPh_3 ligands and a hydride mutually *cis* to these two ligands. Although two other isomers are possible with a *fac*- $\text{Ru}(\text{PPh}_3)_2(\text{CO})$ substructure, we favor the one that involves the direct addition of CO to the vacant site of **2**. This is different

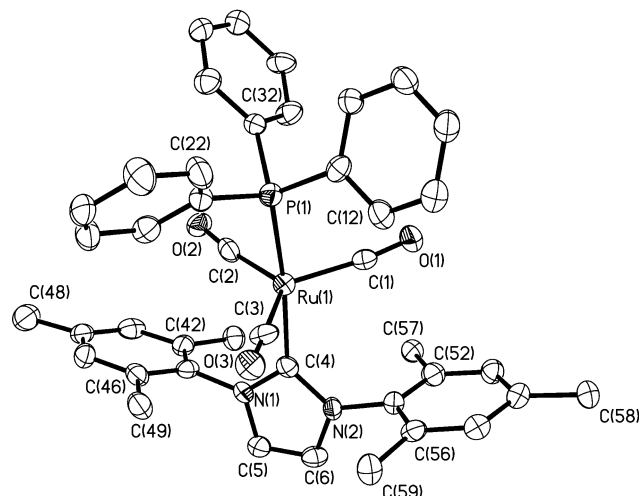


Figure 2. X-ray crystal structure of $\text{Ru}(\text{CO})_3(\text{IMes})(\text{PPh}_3)$ (**5**).

Scheme 3. Reactions of $\text{RuH}(\text{IMes-H})(\text{PPh}_3)_2$ with Carbon Monoxide

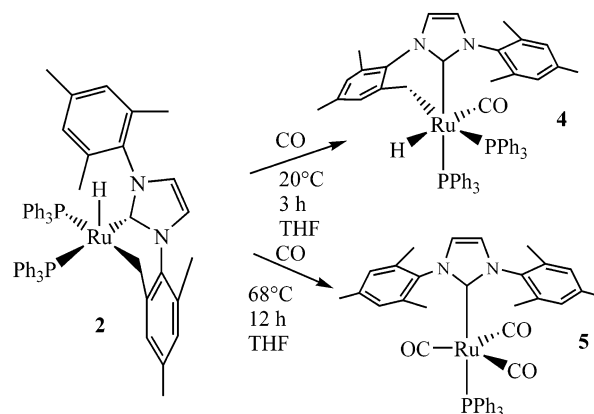


Table 3. Selected Bond Lengths and Angles in $\text{Ru}(\text{CO})_3(\text{IMes})(\text{PPh}_3)$ (**5**)

Bond Lengths (Å)			
Ru(1)–C(3)	1.91(2)	Ru(1)–C(1)	1.92(2)
Ru(1)–C(2)	1.93(2)	Ru(1)–P(1)	2.341(3)
Ru(1)–C(4)	2.12(2)	C(5)–C(6)	1.35(2)
Bond Angles (deg)			
C(3)–Ru(1)–C(1)	122.9(5)	C(2)–Ru(1)–P(1)	88.4(3)
C(2)–Ru(1)–C(1)	110.1(4)	C(3)–Ru(1)–P(1)	87.3(3)
C(2)–Ru(1)–C(3)	126.8(5)	C(4)–Ru(1)–P(1)	171.4(3)
C(3)–Ru(1)–C(4)	84.8(4)	N(1)–C(4)–N(2)	103.5(8)
C(2)–Ru(1)–C(4)	93.7(4)	C(1)–Ru(1)–C(4)	96.3(4)
C(1)–Ru(1)–P(1)	90.8(3)		

from the isomer reported earlier with the *OC-53* configuration (Chart 1).¹⁵

The reaction of **2** with an excess of CO at higher temperature resulted in the intramolecular reductive elimination of a C–H bond from the cyclometalated methyl group, coordination of three carbon monoxide molecules, and loss of a phosphine ligand to form $\text{Ru}(\text{CO})_3(\text{IMes})(\text{PPh}_3)$ (**5**; Scheme 3). Complex **5** is a yellow solid that is stable in air indefinitely, soluble in THF, benzene, and diethyl ether, and insoluble in hexanes. The crystal structure of $\text{Ru}(\text{CO})_3(\text{IMes})(\text{PPh}_3)$ (Figure 2, Table 3) has a slightly distorted trigonal bipyramidal coordination geometry, similar to that of the analogous complex $\text{Ru}(\text{CO})_3(\text{PPh}_3)_2$, which also crystallized as the

(24) Coalter, J. N.; Bollinger, J. C.; Huffman, J. C.; Werner-Zwanziger, U.; Caulton, K. G.; Davidson, E. R.; Gerard, H.; Clot, E.; Eisenstein, O. *New J. Chem.* **2000**, *24*, 9–26.

(25) Winter, R. F.; Hornung, F. M. *Inorg. Chem.* **1997**, *36*, 6197–6204.

(26) Scholl, M.; Trnka, T. M.; Morgan, J. P.; Grubbs, R. H. *Tetrahedron Lett.* **1999**, *40*, 2247–2250.

(27) Weskamp, T.; Schattenmann, W. C.; Spiegler, M.; Herrmann, W. A. *Angew. Chem., Int. Ed. Engl.* **1998**, *37*, 2490–2493.

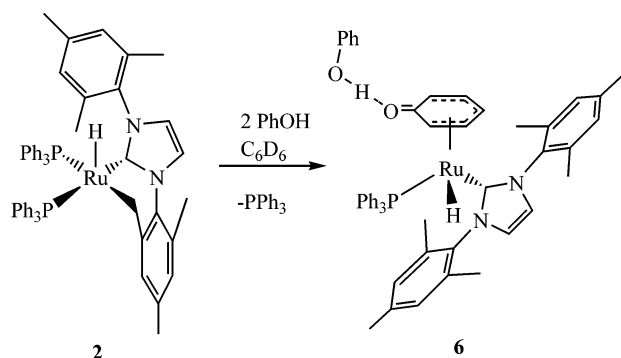
(28) Grushin, V. V. *Acc. Chem. Res.* **1993**, *26*, 279–286.

(29) Owen, M. A.; Pye, P. L.; Piggott, B.; Capparelli, M. V. *J. Organomet. Chem.* **1992**, *434*, 351–362.

(30) Trnka, T. M.; Morgan, J. P.; Sanford, M. S.; Wilhelm, T. E.; Scholl, M.; Choi, T. L.; Ding, S.; Day, M. W.; Grubbs, R. H. *J. Am. Chem. Soc.* **2003**, *125*, 2546–2558.

(31) Hitchcock, P. B.; Lappert, M. F.; Pye, P. L.; Thomas, S. *J. Chem. Soc., Dalton Trans.* **1979**, 1929–1942.

(32) Jazzar, R. F. R.; Bhatia, P. H.; Mahon, M. F.; Whittlesey, M. K. *Organometallics* **2003**, *22*, 670–683.

Scheme 4. Reaction of **2** with Phenol

THF solvate.³³ The three carbonyl ligands do not form an exact equatorial triangle. Rather, the two carbonyl ligands (C2–O2 and C3–O3) that are situated directly above the large mesityl rings of the carbene ligand (see Figure 2) are pointed upward to relieve steric repulsions.

The ³¹P NMR spectrum of **5** has a singlet at 55.72 ppm. The ¹H NMR spectrum has no signal in the hydride region, confirming the loss of hydride. The unsymmetrical structure of **5** in the solid state results in three IR absorptions by CO in the region of 1850–1965 cm⁻¹. The bis(phosphine) complex Ru(CO)₃(PPh₃)₂ in solution has only one IR-active asymmetric mode at 1895 cm⁻¹.³⁴

Sometimes **5** formed under mild reaction conditions that should have lead to **4**. An acidic impurity that protonates **2**, thereby catalyzing the reductive elimination of the Ru–C bond, might be responsible.

The reactivity of the Ru–C cyclometalated bond was probed by reaction with the weak acid phenol. The reaction of phenol with **2** in benzene resulted in the protonation of the cyclometalated methyl group from the IMes ligand, followed by η⁵ coordination of the phenoxide moiety and loss of phosphine to form complex **6** (Scheme 4). Complex **6** is an air-sensitive yellow solid, soluble in THF, benzene, and diethyl ether and insoluble in hexanes.

Complex **6** has a distorted-tetrahedral coordination geometry with four different ligands, thereby making it chiral (Figure 3). A phenoxide ligand is η⁵ bonded to Ru(II) and hydrogen bonded via the oxygen to a neutral phenol molecule in the crystal lattice. The Ru(1)–C(4) distance is much longer than the other Ru–C distances to the η⁵-PhO ligand (Table 4). Two complexes with a similar structure are (η⁵-C₆H₅O)RuH(PPh₃)₂³⁵ and (η⁵-C₆H₅O)RuH(PCy₃)₂.³⁶ One of the mesityl rings is stacked against a phenyl ring with a ring–ring spacing of about 3.4 Å, the same as the interlayer distance in graphite.

The consequence of the chirality of the complex can be seen in the ¹H NMR spectrum. The six methyl resonances of the IMes ligand are inequivalent. Further evidence for π-coordination of the aryloxide ligand is indicated by the upfield shift of the aromatic proton resonances to between 4.9 and 5.8 ppm in the ¹H NMR

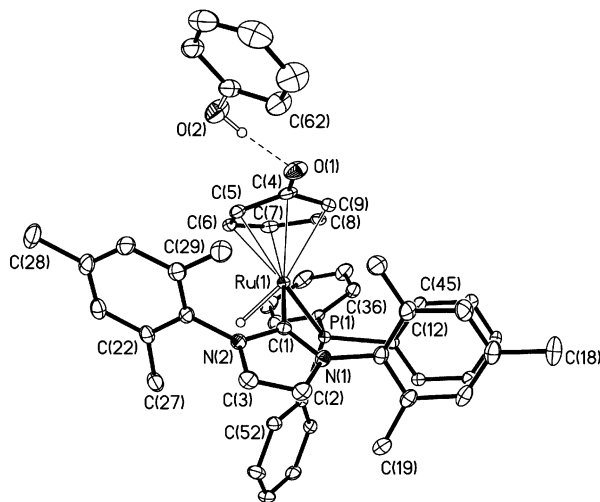
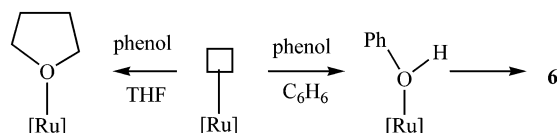


Figure 3. X-ray crystal structure of **6**.

Table 4. Selected Bond Lengths and Angles for **6**

Bond Lengths (Å)			
Ru(1)–H(1Ru)	1.60(2)	Ru(1)–C(6)	2.204(2)
Ru(1)–C(1)	2.087(2)	Ru(1)–C(8)	2.224(2)
Ru(1)–P(1)	2.2799(6)	Ru(1)–C(9)	2.358(2)
Ru(1)–C(7)	2.221(2)	Ru(1)–C(5)	2.304(2)
Ru(1)–C(4)	2.566(2)	C(4)–O(1)	1.275(3)
Bond Angles (deg)			
H(1Ru)–Ru(1)–C(1)	79.6(8)	P(1)–Ru(1)–C(4)	145.19(7)
P(1)–Ru(1)–C(1)	97.52(6)	C(1)–Ru(1)–C(4)	96.82(8)
H(1Ru)–Ru(1)–P(1)	77.8(8)	H(1Ru)–Ru(1)–C(4)	136.2(8)

Scheme 5. Inhibition by THF of the Reaction of **2** with Phenol

spectrum and of five of the six carbon atoms to between 97 and 67 ppm in the ¹³C NMR. The carbon attached to oxygen has carbonyl character and appears at 161.5 ppm.

Significantly, there is no reaction of **2** with phenol when the solvent is changed from benzene to THF. The reason may be that THF coordinates to the vacant coordination site of **2**, and this prevents phenol from coordinating and reacting (Scheme 5). The reaction in benzene may proceed via an O-bonded phenol intermediate in which the phenol becomes acidic due to complexation. This acid can then break the cyclometalated bond between IMes and ruthenium to initiate the reaction. Recently an O-bonded phenol complex containing two IMes ligands on ruthenium has been reported.³²

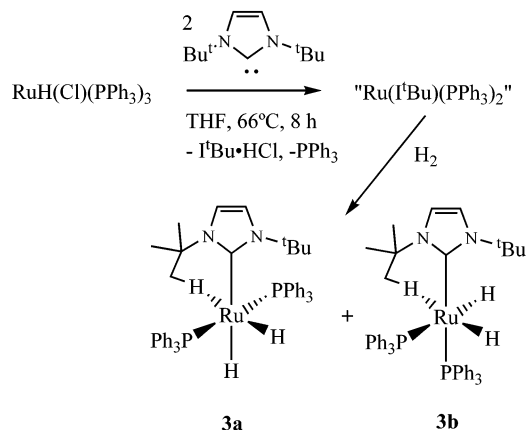
Ruthenium Complex of a Carbene with *tert*-Butyl Groups. Unlike the reactions in Scheme 2 that go directly to a red, cyclometalated product, the reaction of RuHCl(PPh₃)₃ with **2** equiv of the carbene I^tBu (1,3-di-*tert*-butylimidazol-2-ylidene) leads to the formation of I^tBuH⁺Cl⁻ and an extremely reactive red solution (Scheme 6). The solution behaves as if it contains “Ru(I^tBu)(PPh₃)₂” (see below), in that it reacts with hydrogen gas to form the new yellow complex RuH₂(I^tBu)(PPh₃)₂ as a mixture of two isomers (**3a,b**). As with IMes or SIMes, attempts to form a bis(carbene) complex with the I^tBu ligand also failed.

(33) Dahan, F.; Sabo, S.; Chaudret, B. *Acta Crystallogr., Sect. C: Cryst. Struct. Commun.* **1984**, *40*, 786–788.

(34) Edwards, A. J.; Leadbeater, N. E.; Lewis, J.; Raithby, P. R. *J. Organomet. Chem.* **1995**, *503*, 15–20.

(35) Cole-Hamilton, D. J.; Young, R. J.; Wilkinson, G. *J. Chem. Soc., Dalton Trans.* **1976**, *19*, 1995.

(36) Christ, M. L.; Sabo-Etienne, S.; Chung, G.; Chaudret, B. *Inorg. Chem.* **1994**, *33*, 5316–5319.

Scheme 6. Synthesis of RuH₂(tBu)(PPh₃)₂ (isomers **3a and **3b**)****Table 5. Selected Bond Lengths and Angles for **3a****

Bond Lengths (Å)			
Ru(1)–H(1Ru)	1.64(3)	Ru(1)–P(1)	2.2803(6)
Ru(1)–H(2Ru)	1.50(2)	Ru(1)–P(2)	2.2876(5)
Ru(1)–H(9A)	1.9	Ru(1)–C(1)	2.118(2)
C(2)–C(3)	1.344(3)		

Bond Angles (deg)			
H(1Ru)–Ru(1)–C(1)	175.1(9)	H(1Ru)–Ru(1)–H(9A)	93(1)
H(2Ru)–Ru(1)–C(1)	100(1)	C(1)–Ru(1)–P(2)	104.60(6)
H(1Ru)–Ru(1)–P(1)	82(1)	C(1)–Ru(1)–P(1)	99.58(6)
H(2Ru)–Ru(1)–P(1)	81(1)	N(1)–C(1)–N(2)	111.4(2)
H(1Ru)–Ru(1)–H(2Ru)	85(1)	P(2)–Ru(1)–P(1)	153.28(2)
H(2Ru)–Ru(1)–H(9A)	170(1)	H(2Ru)–Ru(1)–P(2)	84(1)
H(1Ru)–Ru(1)–P(2)	74.9(9)	H(9A)–Ru(1)–P(2)	105(1)

Complex **3** as a mixture of isomers is an air-sensitive yellow solid, soluble in THF, benzene, and diethyl ether and insoluble in hexanes. The structure of **3a** has been determined by single-crystal X-ray diffraction and verified by NMR, while the structure of **3b** has been inferred by use of NMR. Complex **3a** has a distorted-octahedral structure where one of the ligands is an agostic methyl hydrogen³⁷ from one of the *tert*-butyl groups of the N-heterocyclic carbene ligand (Table 5 and Figure 4). The Ru(1)···H(9A) distance (1.93 Å), Ru(1)···C(9) distance (2.63 Å), and Ru···H–C angle (127°) are similar to those of the following ruthenium complexes with agostic methyl groups: [(tBu₂PCH₂PtBu₂)(CHPh)Ru]₂-(μ₂-Cl)₃,³⁸ [Ru(PPh₂CH₂CH₂PPh₂)(HB(N₂C₃H₅Pr₂)₃)O₃-SCF₃],³⁹ RuCl₂{PPh₂(2,6-Me₂C₆H₃)₂},⁴⁰ and [RuPh(CO)-(P^tBu₂Me)₂]BAR⁴.⁴¹ The P(1)–Ru(1)–P(2) bond angle of only 153.28(2)° is due mainly to steric effects. This leaning of the PPh₃ ligands toward the small hydride ligands is a common feature of dihydride complexes that is also observed, for example, in *cis,trans*-Ru(H)₂(PPh₃)₂-(*R,R*-dach)⁴² (P–Ru–P = 158.21(3)°) and in complexes of the type *cis,trans*-[M(H)₂(PPh₃)₂(L)₂]⁺ (M = Rh, Ir, L = various ligands).⁴³ The two hydrides are in a *cis*

(37) Brookhart, M.; Green, M. L. H. *J. Organomet. Chem.* **1983**, *250*, 395–408.

(38) Hansen, S. M.; Rominger, F.; Metz, M.; Hofmann, P. *Chem. Eur. J.* **1999**, *5*, 557–566.

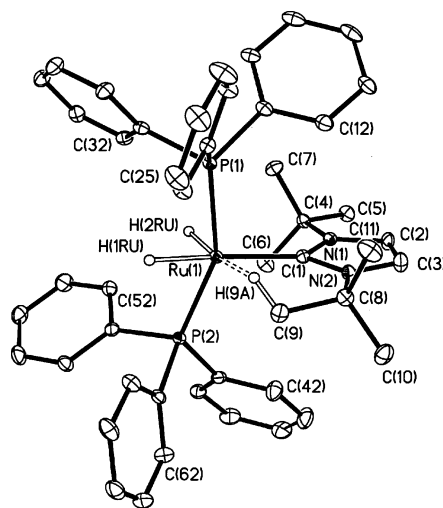
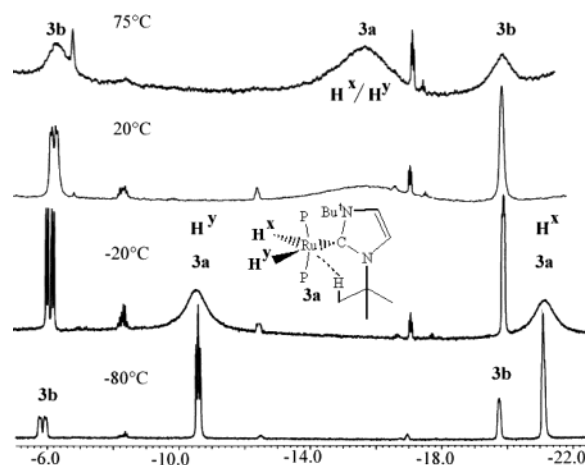
(39) Takahashi, Y.; Hikichi, S.; Akita, M. *Organometallics* **1999**, *18*, 2571–2573.

(40) Baratta, W.; Herdtweck, E.; Rigo, P. *Angew. Chem., Int. Ed.* **1999**, *38*, 1629–1631.

(41) Huang, D. J.; Streib, W. E.; Bollinger, J. C.; Caulton, K. G.; Winter, R. F.; Scheiring, T. *J. Am. Chem. Soc.* **1999**, *121*, 8087–8097.

(42) Abdur-Rashid, K.; Lough, A. J.; Morris, R. H. *Organometallics* **2000**, *19*, 2655–2657.

(43) Survey of the Cambridge Crystallographic Database.

**Figure 4. X-ray structure of RuH₂(tBu)(PPh₃)₂ (isomer **3a**).****Figure 5. ¹H VT NMR spectrum (500 MHz) in the hydride region of a mixture of **3a** and **3b** in toluene-*d*₈.**

configuration, with H(2Ru) being *trans* to the coordinated C–H bond and H(1Ru) being *trans* to the carbene ligand.

The two isomers **3a,b** are produced in a 7:3 ratio according to the ³¹P NMR spectrum. The major isomer has two equivalent phosphorus nuclei (singlet at 64.3 ppm), a feature that is consistent with the structure determined by crystallography. The minor isomer (see Scheme 6) has inequivalent phosphorus nuclei, as represented by doublet signals at 51.4 and 62.7 ppm.

The low-temperature ¹H NMR spectra also support the structures shown in Scheme 6. The spectrum at –80 °C has a triplet at –10.6 ppm and a broadened triplet at –21.1 ppm assigned to **3a** and a doublet of doublets at –5.8 ppm (²J_{HP}^{trans} = 83.5 Hz, ²J_{HP}^{cis} = 30.5 Hz) and a broad singlet at –19.75 ppm assigned to **3b** (Figure 5). The triplet signals for **3a** are consistent with the crystal structure, with both hydrides *cis* to two equivalent phosphines. No significant hydride–hydride coupling is observed, due to their *cis* configuration. The broadness of the triplet at –21.14 ppm may be due to this hydride being situated *trans* to the coordinated C–H bond that is undergoing exchange with other C–H bonds of the coordinated *tert*-butyl group by rotations within this group. The other hydride is unaffected, due to its *cis* orientation with respect to the agostic hydro-

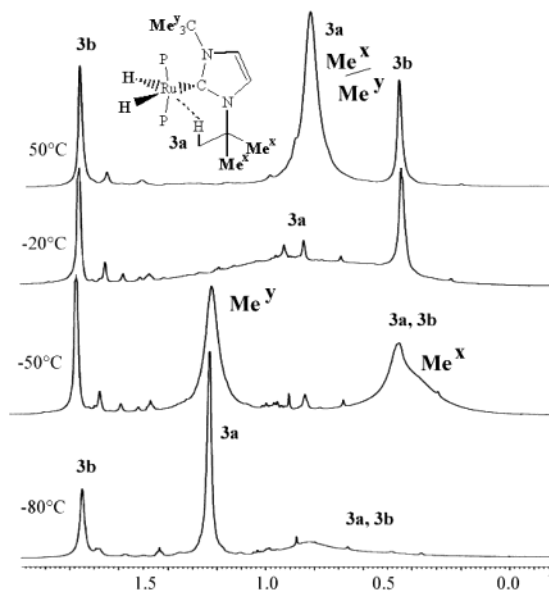
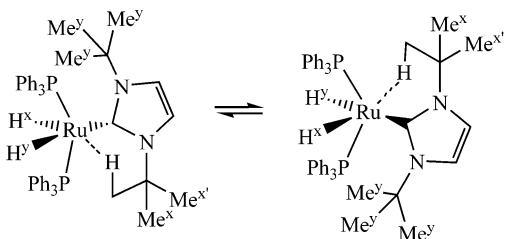


Figure 6. ^1H VT NMR spectrum (500 MHz) in the methyl region of a mixture of **3a** and **3b** in toluene- d_8 .

Scheme 7. “Windshield-Wiper” Fluxional Exchange of Coordinated *tert*-Butyl Groups in **3a**



gen. The signal for the hydride trans to phosphorus in isomer **3b** (Scheme 6) is likely to be the one at -5.9 ppm, with a hydride–phosphorus splitting of 83.5 Hz. The broadness of the triplet at -19.8 ppm for the other hydride of **3b** can be rationalized in a manner similar to the triplet at -21.1 ppm of **3a**: the hydride is positioned trans to the agostic hydrogen.

The hydride signals of **3a** coalesce at approximately 10 °C into a broad signal at -16 ppm due to a “windshield wiper” process involving the interchange of coordinated and free *tert*-butyl groups (Scheme 7), while the signals due to **3b** remain distinct up to 50 °C (Figure 5).

The methyl resonances in the ^1H NMR spectrum of both isomers of **3** in toluene- d_8 (Figure 6) undergo line-shape changes that are evidence for the presence of coordinated and free *tert*-butyl groups and of the “windshield-wiper” motion (Scheme 7). At -80 °C the methyl groups of the free *tert*-butyl group of **3a** have a sharp resonance at 1.24 ppm, while those on the coordinated *tert*-butyl group are completely broadened out by exchange among free and coordinated C–H bonds. The coordinated hydrogen is expected to have a negative chemical shift,³⁸ while the free methyl hydrogens should appear at about 1 ppm. This fluxional process of exchange within the coordinated *tert*-butyl group could not be frozen out in this study because of increases in viscosity and the freezing of the toluene solvent at lower temperatures. At -50 °C these two types of proton chemical shifts average to give a broad methyl reso-

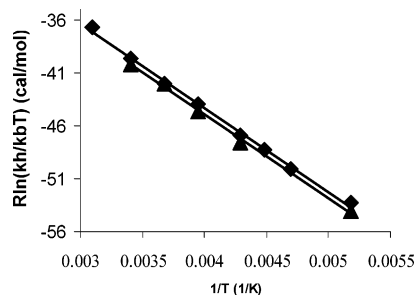


Figure 7. Eyring plot from data obtained from rate constants from (♦) the ^1H NMR hydride signals and (▲) the ^1H NMR methyl signals. Solid lines are from least-squares fits.

Table 6. Rate Constants (s^{-1}) from the DNMR4 Fitting of NMR Spectra of **3a in the Hydride Region (Figure 5) and Methyl Region (Figure 6)**

temp (°C)	rate constant (s^{-1})	
	hydride region	methyl region
-80	9	6
-60	50	
-50	130	
-40	275	190
-20	1300	900
-1	3600	3750
20	13000	10000
50	63000	

nance for the coordinated *tert*-butyl group at 0.5 ppm (Figure 6). However, even at this temperature the “windshield-wiper” motion causes a broadening of the methyl resonances at 1.2 and 0.5 ppm and at higher temperatures leads to a coalescence of the peaks so that in the range of 0 – 70 °C one broad peak is observed for all of the *tert*-butyl methyl hydrogens.

The methyl groups of the minor isomer, **3b**, also have two types of signals—one for the coordinated *tert*-butyl group at 0.4 ppm and one for the free *tert*-butyl group at 1.8 ppm (Figure 6). Like isomer **3a**, the exchange among free and coordinated C–H bonds of the coordinated *tert*-butyl group causes an extreme broadening of the peak at 0.4 ppm at low temperatures. Unlike isomer **3a**, there is no averaging of the free and coordinated methyl resonances to high temperature. This is not unexpected, since this process could only happen in **3b** if the whole carbene ligand rotated by 180° , a higher energy process than the windshield-wiper process of **3a**.

The energy of the windshield-wiper process was determined by simulations of the VT NMR spectra using the program DNMR4. NMR fitting simulations were performed on both methyl and hydride regions of the NMR spectra to determine whether the same process was occurring during the fluxional transition. Simulations yielded rate constants ($1/\tau$) at varying temperatures for the transition (Table 6). The rate constants were used to compose an Eyring plot of $R \ln(k_h/k_b T)$ vs $1/T$ (Figure 7), from which activation energy data could be determined (Table 7).

Within error, the activation energy components are in very good agreement for the windshield-wiper process, whether observed via the methyl or hydride resonances (Table 7). The energy of the fluxional process is ca. 11.7 kcal/mol, which is within the NMR energy range for observable transitions. The enthalpy of activa-

Table 7. Activation Energy Data Determined from the VT ^1H NMR Spectra of 3a

	methyl region	hydride region
ΔH^\ddagger (kcal/mol)	7.97	7.97
ΔS^\ddagger (cal/(K/mol))	-12.5	-13.0
ΔG^\ddagger (kcal/mol)	11.7	11.8

tion of 8 kcal/mol might represent approximately the energy of the decoordination of the agostic $\text{Ru}\cdots\text{HC}$ bond. Energies in the range of 7–15 kcal/mol for agostic interactions have been reported.³⁹ However, the entropy of activation is negative, possibly an argument for a concerted coordination and decoordination process.

The red, very reactive intermediate “ $\text{Ru}(\text{I}^t\text{Bu})(\text{PPh}_3)_2$ ” of Scheme 6 is soluble in all organic solvents at hand, including THF, ether, and hexanes. A solution in C_6D_6 gave only trace hydride resonances in the ^1H NMR spectrum at room temperature. The ^{31}P NMR spectrum of the THF solution containing the intermediate under Ar has two doublets at -30.3 and 43.2 ppm ($^2J_{\text{PP}} = 22$ Hz) as well as a peak for free PPh_3 and several other minor peaks. This indicates that the major component has two inequivalent phosphines in a cis configuration. The signal at -30.3 ppm is indicative of a triphenylphosphine molecule that has undergone cyclometallation of one of the phenyl rings.⁴⁰ Upon addition of hexanes in an attempt to isolate the complex, the yellow compound $\text{RuH}_2(\text{PPh}_3)_4$ ⁴¹ precipitated out of the red solution. This suggests that the intermediate is unstable with respect to a disproportionation of phosphine ligands between two or more complexes.

Conclusion

The reaction of $\text{RuHCl}(\text{PPh}_3)_3$ with IMes and SIMes results in the cyclometallation of a methyl group of the

carbene ligand in the complexes $\text{RuH}(\text{SIMes-H})(\text{PPh}_3)_2$ and $\text{RuH}(\text{IMes-H})(\text{PPh}_3)_2$. The reaction with I^tBu appears to proceed via cyclometallation of the phosphine ligand; however, after reaction with H_2 , the dihydride complex $\text{Ru}(\text{H})_2(\text{I}^t\text{Bu})(\text{PPh}_3)_2$ is isolated. In this complex a methyl of the carbene ligand is coordinated but the C–H bond is agostic and not broken. There is an interesting windshield wiper exchange of coordinated *tert*-butyl groups occurring in one isomer of this molecule with a free energy of activation of approximately 11.8 kcal/mol. The complex $\text{RuH}(\text{IMes-H})(\text{PPh}_3)_2$ reacts with CO to give an isomer of $\text{RuH}(\text{CO})(\text{IMes-H})(\text{PPh}_3)_2$ different from that observed by Whittlesey and co-workers. The new complex $\text{Ru}(\text{CO})_3(\text{PPh}_3)(\text{IMes})$ forms upon further reaction with CO. The cyclometalated IMes ligand of $\text{RuH}(\text{IMes-H})(\text{PPh}_3)_2$ can be relatively easily protonated by phenol, and the resulting complex $\text{RuH}(\text{C}_6\text{H}_5\text{O}\cdot\text{HOPh})(\text{IMes})(\text{PPh}_3)$ has an interesting η^5 -bonded phenoxide group. Larger ligands such as IMes and PPh_3 do not react with **2**, even though it is coordinatively unsaturated.

Acknowledgment. The NSERC is thanked for a discovery grant to R.H.M. and Johnson Matthey is acknowledged for a loan of ruthenium trichloride.

Supporting Information Available: Figures giving simulations of the VT NMR spectra and crystallographic data as CIF files. This material is available free of charge via the Internet at <http://pubs.acs.org>.

OM034178G